Available online at www.sciencedirect.com
SCIENCE DIRECT®
Polyhedron 22 (2003) 3547–3553
POLYHEDRON
www.elsevier.com/locate/poly

Synthesis and crystal structure of maleonitriledithiolate metal complexes with *N*-methylacridine as cations

Li-Fen Yang, Zheng-He Peng *, Gong-Zhen Cheng, Shie-Ming Peng

Department of Chemistry, Wuhan University, Wuhan 430072, PR China

Received 17 March 2003; accepted 7 July 2003

Abstract

The synthesis of $[N\text{-MeA}]_2[M(mnt)_2]$ (*N*-MeA = *N*-methylacridine; M = Ni (II), Zn (II), Cu (II) and Cd (II); mnt = maleonitriledithiolate) and crystal structure analysis of the Ni (**1**) and Zn (**2**) complexes are reported. The conductivities of almost all the complexes under 4 MPa pressure are above 10^{-5} S cm^{-1}, which are characteristic of intrinsic semi-conductors. The complexes exhibit charge transfer transitions in both their absorption spectra and fluorescence spectroscopy.

Keywords: Electrical conductivities; Crystal structures; Charge transfer transitions; Fluorescence spectroscopies; Molar conductances

1. Introduction

Maleonitriledithiolate (mnt^{2-}) complexes have been widely studied mainly because the highly delocalized system extending out to the cyanine groups at the periphery displays a versatile set of structural, chemical and physical properties. Transition metal complexes of similar dithiolenes such as mnt^{2-} [1], $dmit^{2-}$ [2] (1,3-dithiol-2-thione-4,5-dithiolate), $dmio^{2-}$ (1,3-dithiol-2-one-4,5-dithiolate) [3] and $dddt^{2-}$ (5,6-dihydro-1,4-dithiin-2,3-dithiolate) [4] have potential applications in the areas of conducting and magnetic materials, dyes, non-linear optics, and catalysis. Undoubtedly, these applications are connected with a combination of functional properties, specific geometries and intermolecular interactions.

Billig et al. [6] synthesized the first divalent transition metal complex containing the mnt ligand as the tetraethylammonium salt. The high charge density on the delocalized π-electron system can interact with different types of counterions, forming different stacking modes in the solid state. This interaction is one of the dominant factors in the determination of the physical properties caused by intermolecular interactions. Therefore, studies on the four-coordinated metal dithiolene salts with different counterions are worthwhile.

Acridine is a heterocyclic compound containing a delocalized π system, and it can be considered as an intermediate between typical closed-shell cations, such as R_4N^+ (R = alkyl) and guanidinium, and typical open-shell cations such as $TTF^{+\cdot}$ and $EDT\text{-}TTF^+$ [2,7].

In the present paper, the synthesis, crystal structure, and conductivity properties of $[N\text{-MeA}]_2[M(mnt)_2]$ complexes are reported, and their UV–Vis spectra and fluorescence properties are also discussed.

2. Experimental

2.1. General materials and techniques

All chemical reagents of A.R. grade were used as supplied without further purification. The sodium salt of the ligand, *cis*-maleonitriledithiolate (Na_2mnt), was prepared according to the published method [5]. [*N*-MeA]I was synthesized as described in the literature [8].

Analyses of C, H, and N were performed on a Perkin–Elmer 240B elemental autoanalyzer. Fluorescence measurements were performed using a Perkin–Elmer LS 55 luminescence spectrometer with 1-cm quartz cuvettes at

* Corresponding author. Tel.: +86-27-872-18504; fax: +86-27-876-47617.
E-mail address: pengzh@chem.whu.edu.cn (Z.-H. Peng).

0277-5387/$ - see front matter © 2003 Elsevier Ltd. All rights reserved.
doi:10.1016/S0277-5387(03)00459-5

room temperature. UV–Vis–Near-infrared spectra were recorded on a Beijing *Puxi* TU-1901 spectrophotometer. Infrared absorption spectra were recorded on a Perkin–Elmer FT-IR spectrometer (KBr pellets, 4000 – 400 cm^{-1}). Proton NMR of **2** was recorded on a Varian Mercury-vx 300 MHz FT-NMR spectrometer. Molar conductance was measured on a DDS-11A conductor using a platinum electrode. Electrical conductivity of pressed pellets of the products was obtained by the four-probe method (except $[N\text{-MeA}]_2[Cu(mnt)_2]$, which used the two-probe method) in the 275–22 K temperature range with copper wires glued on the pellet surfaces. Pellets of 0.5–1.2 mm thickness were obtained upon applying 4 MPa pressure to the sample for 5 min. The main instruments for conductivity measurement were: 2400 Source Meter (Keithley), 2182 Nanovolmeter, 7001 Switch System, and 340 Temperature Controller (Lakeshore). A 0.06 μA current was used in this experiment.

2.2. Synthesis of complexes

2.2.1. $[N\text{-}MeA]_2[Ni(II)(mnt)_2]$ (**1**)

Under an N_2 atmosphere, a solution of $NiCl_2 \cdot 6H_2O$ (0.24 g, 1.0 mmol) and [*N*-MeA]I (0.64 g, 2.0 mmol) in 30 ml methanol was added dropwise to a solution of Na_2(mnt) (0.38 g, 2.0 mmol) in 20 ml methanol with stirring, and a brown solid was precipitated immediately. After 2.5 h, the solid was filtered off carefully, and washed with water, methanol, and ether. This crude product was recrystallized from DMF/ether and dried under vacuum over P_2O_5 at 100 °C for at least 24 h. Yield 0.44 g (60.6%) of dark brown powder: m.p. >250 °C (decomp.); elemental analysis Calc. (%) for $C_{36}H_{24}N_6S_4Ni$: C, 59.42; H, 3.32; N, 11.55. Found: C, 58.37; H, 3.35; N, 11.23%. IR data (cm^{-1}, KBr pellet), 2195 (s), 1620 (s), 1579 (m), 1543 (m), 1489 (vs), 1463 (m), 1396 (m), 1269 (w), 1192 (w), 1148 (s), 1105 (w), 1036 (w), 971 (w), 941 (w), 862 (w), 834 (w), 769 (m), 730 (m), 727 (m), 601 (w).

Single crystals were grown by slow diffusion of methanol to the salt in acetonitrile. A black cube-shaped single crystal of suitable size for X-ray diffraction was found in a week.

2.3. $[N\text{-}MeA]_2[Zn(II)(mnt)_2]$ (**2**)

The procedure was similar to the previous one. A 10 ml methanol solution of $Zn(OAc)_2 \cdot 2H_2O$ (0.22 g, 1.0 mmol) was added slowly to a 20 ml methanol solution of Na_2(mnt) (0.38 g, 2.0 mmol) with stirring under a nitrogen atmosphere. After stirring for 30 min, a solution of [*N*-MeA]I (0.64 g, 2.0 mmol) in 30 ml methanol was added dropwise. A purple microcrystalline precipitate with metallic lustre was formed immediately. The mixture was stirred for another 2 h. Then the solid was filtered off, recrystallized from acetonitrile and dried under vacuum over P_2O_5 at 100 °C for at least 24 h. Yield 0.32 g (44.0%) of purple metallic colored microcrystal. Elemental analysis: Calc. (%) for $C_{36}H_{24}N_6S_4Zn$: C, 58.88; H, 3.29; N, 11.45. Found: C, 60.97; H, 3.57; N, 11.60%. ^1H NMR (acetonitrile-d_3): 4.78 (s), 7.10 (s), 7.84 (s), 8.02 (t), 8.40 (t), 8.52 (t); IR data (cm^{-1}, KBr pellet), 2360 (w), 2196 (s), 1623 (vs), 1578 (w), 1542 (s), 1441 (m), 1398.3 (m), 1390 (m), 1267 (w), 1206 (w), 1146 (s), 1114 (m), 1037 (w), 862 (w), 769 (m), 740 (s), 601 (w).

Single crystals of suitable size for X-ray diffraction were grown by the same procedure as for **1**.

2.3.1. $[N\text{-}MeA]_2[Cu(II)(mnt)_2]$ (**3**)

A methanol solution of $CuCl_2 \cdot 2H_2O$ (0.17 g, 1.0 mmol) was added dropwise to a 10 ml methanol solution of Na_2(mnt) (0.38 g, 2.0 mmol) with stirring under nitrogen atmosphere. Then [*N*-MeA]I (0.65 g, 2.0 mmol) in 20 ml methanol was added dropwise. A dark-green precipitate was formed immediately. Then it was stirred for another 2 h. This solid was filtered off, recrystallized from DMF/ether, and dried under vacuum over P_2O_5 at 100 °C for 24 h. Yield 0.34 g (46.1%) of dark-green powder. Elemental analysis: Calc. (%) for $C_{36}H_{24}N_6S_4Cu$: C, 59.03 ; H, 3.28 ; N, 11.48. Found: C, 55.06; H, 3.20; N, 11.92%. IR data (cm^{-1}, KBr pellet) 2922.1 (w), 2196 (s), 1578 (m), 1542 (m), 1468 (vs), 1396 (m), 1267 (w), 1149 (s), 1111 (m), 1034 (w), 974 (w), 945 (w), 771 (m), 739 (s), 601 (w).

2.3.2. $[N\text{-}MeA]_2[Cd(II)(mnt)_2]$ (**4**)

The procedure was similar to the previous ones. A solution of $CdCl_2 \cdot 2.5H_2O$ (0.12 g, 0.5 mmol) was added to a 20 ml methanol solution of Na_2(mnt) (0.19 g, 1.0 mmol) with stirring under nitrogen atmosphere. After 0.5 h stirring, [*N*-MeA]I (0.32 g, 1.0 mmol) in 30 ml methanol was added dropwise to it. A purple precipitate was formed immediately. The reaction was continued for 2 h. Then this crude product was filtered off and recrystallized from DMF/ether. The filtered substance was a brown solid mixed with some green impurities. Then it was redissolved in acetone and filtered. The filtrate was concentrated by rotary evaporation. The final product was recrystallized from acetone/ether. The compound was dried under vacuum over P_2O_5 at 100 °C for 24 h. Yield 0.46 g (58.4%) of purple powder. Elemental analysis: Calc. (%) for $C_{36}H_{24}N_6S_4Cd$: C, 55.34; H, 3.10; N, 10.75. Found: C, 56.42; H, 3.38; N, 10.71%. IR data (cm^{-1}, KBr pellet) 3106 (w), 2196 (s), 1623 (vs), 1579 (m), 1542 (s), 1465 (w), 1435 (s), 1397 (9), 1268 (w), 1206 (w), 1145 (s), 1113 (s), 1305 (w), 964 (w), 860 (w), 769 (m), 739 (s), 601 (w).

2.4. Structure determination and refinement

Crystal data and details of the structure determination of compounds **1** and **2** are given in Table 1. Single-

Table 1
Crystal data and structure refinement of single crystals **1** and **2**

	1	**2**
Empirical formula	$C_{36}H_{24}N_6S_4Ni$	$C_{36}H_{24}N_6S_4Zn$
Formula weight	727.56	734.22
Temperature (K)	291(2)	291(2)
Wavelength (Å)	0.71073	0.71073
Crystal system	monoclinic	tetragonal
Space group	*P*2(1)/*c*	*P*-42(1)/*c*
Unit cell dimensions		
a (Å)	10.684(2)	8.043(1)
b (Å)	7.391(2)	8.043(1)
c (Å)	20.651(4)	26.771(5)
α (°)	90	90
β (°)	90.29(3)	90
γ (°)	90	90
Volume (Å^3)	1630.6(6)	1731.8(5)
Z	2	2
Calculated density (Mg/m^3)	1.482	1.408
Absorption coefficient (mm^{-1})	0.889	0.986
F(0 0 0)	748	752
Crystal size (mm)	0.28 × 0.28 × 0.20	0.25 × 0.20 × 0.20
Theta range for data collection (°)	1.91–27.51	1.52–27.58
Index ranges	$0 \leqslant h \leqslant 13$, $-9 \leqslant k \leqslant 9$, $-25 \leqslant l \leqslant 26$	$-10 \leqslant h \leqslant 0$, $-10 \leqslant k \leqslant 10$, $-32 \leqslant l \leqslant 33$
Reflections collected/unique	4605/2794 [$R_{int} = 0.0348$]	4992/1680 [$R_{int} = 0.0692$]
Refinement method	full-matrix least-squares on F^2	full-matrix least-squares on F^2
Data/restraints/parameters	2794/0/215	1680/0/112
Goodness-of-fit on F^2	1.059	1.118
Final *R* indices [$I > 2\sigma(I)$]	$R1 = 0.0392$, $wR2 = 0.0954$	$R1 = 0.0485$, $wR2 = 0.0961$
R indices (all data)	$R1 = 0.0531$, $wR2 = 0.1002$	$R1 = 0.0697$, $wR2 = 0.1025$
Extinction coefficient	0.0019(7)	0.0032(13)
Largest diffraction peak and hole (e Å^{-3})	0.362 and −0.354	0.174 and −0.330

crystal X-ray diffraction measurements were carried out with a Rigaku RAXIS-IV imaging plate using graphite monochromated Mo Kα radiation ($\lambda = 0.71073$ Å) at 291(2) K. The structures were solved by direct methods and expanded using Fourier techniques. The non-hydrogen atoms were refined anisotropically. The hydrogen atoms in **2** were introduced in idealized calculated positions. All calculations were performed with the SHELXTL 97 programs.

3. Results and discussion

3.1. Descriptions of the crystal structures

3.1.1. X-ray structure of compound *1*

The crystal structure of **1** is shown in Fig. 1, and its stacking arrangement along the *b* axis displayed in Fig. 2. The coordination bond distance and bond angles of compounds **1** and **2** are presented in Table 2. Both cations and anions in **1** are essentially planar, and their

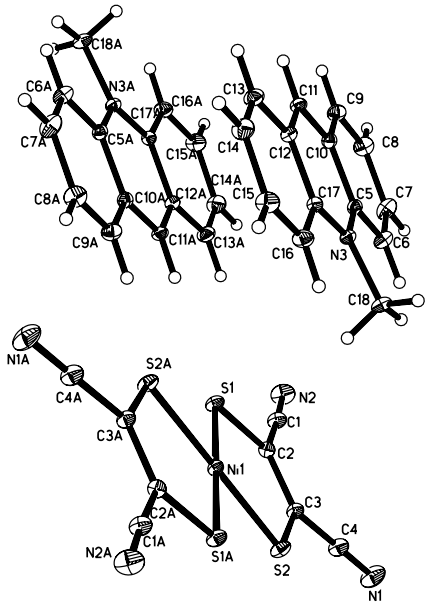

Fig. 1. The crystallographically independent unit with atomic labeling scheme of **1**.

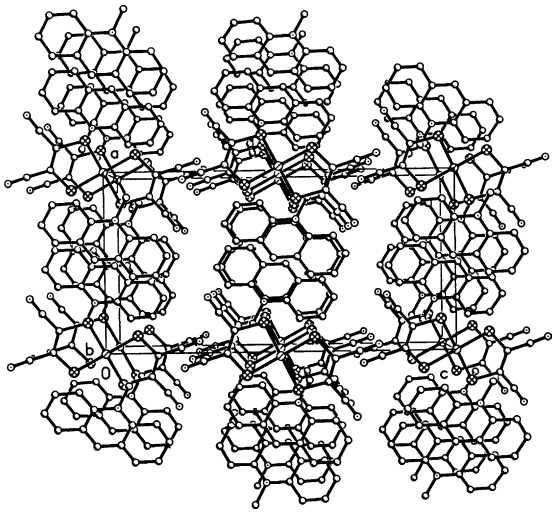

Fig. 2. The stacking arrangement of **1** along the *b* axis.

arrangement can be best described as a mixed stack of dication–anion fragments without short cation–anion interstack contacts. The $[Ni(mnt)_2]^{2-}$ units at the apices are parallel to each other, while those in the interior of unit are tilted by about 45°. The dications are parallel to each other with reverse direction, which may be related with the electron–electron repulsion interaction on the N-atoms.

In this compound, bond lengths of the four coordination bonds are not identical, as most $[Ni(mnt)_2]^{2-}$ derivatives show [9]. The bond lengths of Ni(1)–S(1) are 2.171(9) Å, while those of Ni(1)–S(2) are 2.174(9) Å. Generally, the Ni–S bond distances are longer than those with *N*-methylphenazinium as the counterion [10], but shorter than those with tetraethyl ammonium as the counterion [11]. These two types of Ni–S bond here are almost perpendicular with the S(1)–Ni–S(2) angle being 91.76(3)°.

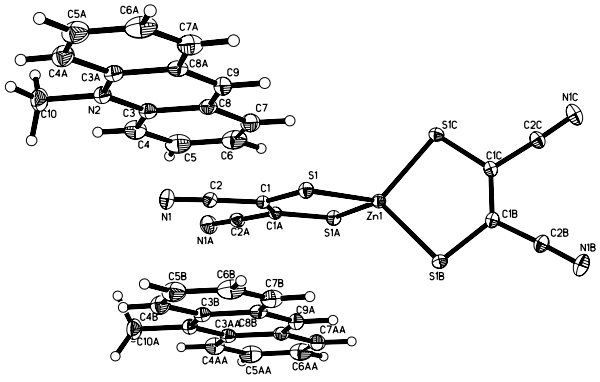

Fig. 3. The crystallographycally independent unit with atomic labeling scheme of **2**.

3.1.2. X-ray structure of compound 2

The crystal structure of **2** and stacking arrangement along the *a* axis of this one are displayed in Figs. 3 and 4, respectively. As in **1**, the structure consists of two cations and one anion. The anion has tetrahedral stereochemistry about the central atom as expected. The crystal structure of compound **2** contains a matrix of cations and anions with hydrogen bonding between the hydrogen atom in the *N*-methylacridine unit and the nitrogen atom in the $[Zn(mnt)_2]^{2-}$ unit. The CH···N distances are typically ca. 2.506 Å, which is shorter than that of the same anion with Ph_4P^+ as counterion, in which the hydrogen bond length of CH···N is 2.85 Å [12]. It should be mentioned that all the Zn–S bonds are identical with the bond length of 2.319(1) Å, unlike the case in compound **1**. The mean Zn–S bond length is longer than that of Ni–S bonds.

In the stacking arrangement of **2** (Fig. 4), for half of the $[Zn(mnt)_2]^{2-}$ units, there are two cations lying above and below it, which are parallel to each other. Unlike the case in **1**, the dications are arranged regularly face-to-face. This can be interpreted by the fact that the

Table 2
Selected bond lengths (Å) and bond angles (°) for crystals **1** and **2**

1		**2**	
Bond lengths			
Ni(1)–S(1)	2.171(9)	Zn(1)–S(1)	2.319(1)
Ni(1)–S(2)	2.174(9)	C(2)–N(1)	1.155(5)
S(1)–C(2)	1.743(3)	C(3)–N(2)	1.381(4)
S(2)–C(3)	1.732(3)	C(10)–N(2)	1.477(6)
C(1)–N(2)	1.146(4)	N(2)–C(3)[c]	1.381(4)
C(4)–N(1)	1.145(4)		
C(5)–N(3)	1.376(3)		
Bond angles			
S(1)–Ni(1)–S(2)	91.76(3)	S(1)[a]–Zn(1)–S(1)	117.44(3)
C(2)–S(1)–Ni(1)	103.67(9)	S(1)[a]–Zn(1)–S(1)[b]	94.50(6)
C(3)–S(2)–Ni(1)	103.60(9)	C(1)–S(1)–Zn(1)	96.63(13)

Symmetry transformations used to generate equivalent atoms.
[a] $y, -x, -z$.
[b] $-x, -y, z$.
[c] $-x+2, -y-1, z$.

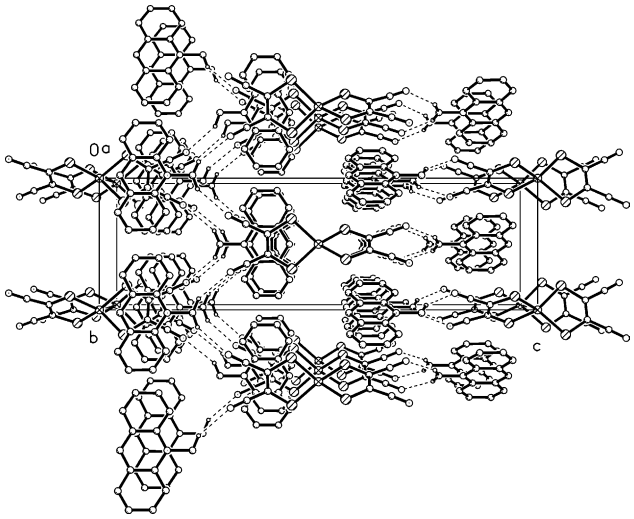

Fig. 4. The stacking arrangement of **2** along the *a* axis.

dications are separated by the $[Zn(mnt)_2]^{2-}$ unit, which greatly reduces the repulsion interactions between pairs of nitrogen atoms. In this complex, the S–S interlayer distance is 6.9 Å, and the acridine plane divides it equally. The dihedral angle between S1–S1A–Zn1–C1–C1A and S1C–S1B–C1B–C1C–Zn1 is 90°.

3.2. IR spectra

The infrared spectra of all the four synthesized compounds are complicated as expected. All show absorptions at ~2195, 1435–1488 and 1144–1149 cm^{-1}, which correspond to ν(C≡N), ν(C=C) and ν(C—S) frequencies of the mnt^{2-} group, respectively. It has been known that the stretching mode of CN groups, i.e., ν(C≡N), is related with the charge (−1 to −3) on the $[M(mnt)_2]^{n-}$ complexes [11]. Comparing the ν(C≡N) stretching mode obtained in this type of complexes with those in $[DT\text{-}TTF]_2[M(mnt)_2]$ salts [13], it can be concluded that four anions in the *N*-methylacridine derivatives have a formal charge of −2. Compared to the IR absorption of the free ligand $Na_2(mnt)$, a perspective positive shift in ν(C=C), insignificant change in ν(C—S) and almost no change in ν(C≡N) in all the complexes indicated that the (S, S) coordinated nature of mnt^{2-} is in a chelating/chelating manner with the C≡N group not involved in bonding [14]. This agrees well with the X-ray results. The strong band at about 1620 cm^{-1} can be assigned to the C=N stretch of *N*-methylacridine cation. The weak band at 2900–3100 cm^{-1} corresponds to the ν(C—H) of the cation.

Table 3
UV–Vis spectra [ϵ (M^{-1} $cm^{-1}10^4$)] and fluorescence spectroscopy of the synthesized compounds (arbitrary intensity)

Compound	UV–Vis		Fluorescence			
	CH_3CN (λ, nm)/ε	DMF (λ, nm)/ε	CH_3CN		DMF	
			λ_{ex} (slit = 10)	λ_{em} (slit = 2.5)	λ_{ex} (slit = 1.0)	λ_{ex} (slit = 1.0)
1	483 (0.28) 443 (0.73) 384 (2.12) 357 (3.58) 342 (1.97) 258 (14.10)	480 (0.39) 381 (0.82) 313sh (3.43) 275 (5.50)	434.0 (194.0)	496.6 (193.6)	402.4 (59.2)	503.6 (39.2)
2	484 (0.31) 442 (0.68) 384 (1.46) 357 (2.36) 340 (1.31) 258 (9.28)	489 (0.17) 401 (1.18) 295 (2.86) 276 (4.25) 267 (4.33)	440.0 (695.0)	488.0 (698.7)	405.2 (204.1)	405.9 (107.1)
3	480 (0.31) 443 (1.65) 418 (0.88) 383 (1.82) 357 (3.20) 342 (1.72) 258 (11.40)	400 (1.21) 380 (1.19) 292sh (4.36) 277 (4.96) 264sh (4.53)	440.0 (71.9)	489.2 (71.5)	402.4 (51.6)	488.0 (19.8)
4	476 (0.51) 443 (0.76) 401 (1.48) 383 (2.48) 358 (2.41) 259 (11.70)	480 (0.11) 401 (1.16) 382 (0.95) 276 (3.19) 267 (3.61)	442.1 (578.2)	486.1 (580.7)	402.9 (286.8)	499.0 (97.3)

3.3. Electronic spectra

The UV–Vis–Near-IR absorption bands of complexes in acetonitrile as well as in DMF are listed in Table 3. The four compounds show similar absorption bands in the same medium, i.e., a set of *B*-bands in the ultraviolet region, which is usually assigned to the interligand π–π^* charge transfer. The UV–Vis spectra also show significant *Q*-bands with maxima absorption at about 480 and 440 nm for acetonitrile media and mainly 480 nm for DMF in the visible region. The absorption near 480 nm, which is characteristic for $[M(mnt)_2]^{2-}$, was considered to originate most likely from L–L, L–M, and M–L transitions [15]. The UV–Vis–Near-IR spectra do not show the ion pair charge-transfer (IPCT) bands, which is different from the $[Co(mnt)_2]^{2-}$ complex as the bipyridium salts [16].

3.4. Fluorescence spectroscopy

The fluorescence data of the compounds in DMF and acetonitrile are shown in Table 3. Emission of the complexes in acetonitrile was measured between 400 and 900 nm. Excitation was performed with wavelengths between 200 and 490 nm. All the complexes display a symmetric emission with λ_{em} at about 500 nm upon excited at 350 nm in acetonitrile, while exhibiting an asymmetric emission in DMF. The emission spectra obtained at these excitation wavelengths did not differ considerably. It is unlikely that emission is due to a d–d transition or L–L transition because mnt^{2-} itself is not photo-emitting [17]. Hence, the observed fluorescence is probably caused by M–L or L–M transitions.

All the four complexes displayed different intensities of emission band in 450–650 nm ranges in the same medium. The fluorescence intensity in the same medium decreases in the following order: Zn > Cd > Ni > Cu. This may be related with the stereo structure of the complexes. The Zn and Cd complexes have the tetrahedron configuration, while that with Ni and Cu metal atoms are planar. The charge transfer excited state of the complexes may be related with the transmetallic state [18]. The collision between the atom of the complexes and the solvent molecule results in loss of energy without radiation, which is influenced by the spatial obstacle [19,20]. Thus the intensity of Ni and Cu complexes is weak, which agrees well with Vogler's results [21]. Comparing the fluorescence spectra of the same complex in different media, it was found that all the fluorescence intensities of the four synthesized compounds are much stronger in acetonitrile than those in DMF.

3.5. Conductivity and molar conductance measurements

As is well known, intermolecular S–S stacking and non-integral oxidation states are important structural and electronic criteria required for the formation of molecular inorganic conductivities. The specific electrical conductivity of the pressed powder pellets depends on the nature of cation and dithiolene ligands. In the present work, conductivity measurements of all the complexes were conducted in the range of 275–22 K. No significant differences were observed between the cooling and heating cycles. The conductivities of the complexes at 275 K are displayed in Table 4. It can be seen that the four salts show specific electrical conductivities at about 10^{-5} S cm^{-1}, which are characteristic of intrinsic semiconductors. The conductivities in these compounds are lower than those with cation to anion ratio of 1:1. In the latter, the conductivity is usually higher than 10^{-3} S cm^{-1} [22]. This may be due to the lack of intermolecular S–S stacking between the cations and anions. However, the conductivities of our synthesized compounds are much higher than those with $[M(phen)_3]^{2-}$ (phen = phenanthroline) as counterions, in which the conductivity is lower than 10^{-10} S cm^{-1} [14]. The specific conductivity herein can be explained by the fact that the arrangement of the donors and acceptors is in a relatively regular manner, as evident from the crystal structures. The low conductivity of **3** may be related with the two-probe method, which increases the resistance of the pressed powder and thus decreases its conductivity.

Table 4
Electrical conductivity at 275 K (S cm^{-1}) and molar conductance (S cm^2 mol^{-1}) of the compounds

Compound	Electrical conductivity	Molar conductance in DMF	Molar conductance in CH_3CN
1	1.88×10^{-5}	173	390
2	1.32×10^{-5}	237	225
3	3.15×10^{-7}	190	267
4	1.94×10^{-5}	148	224

Molar conductances of the four synthesized compounds are also shown in Table 4. It can be seen that molar conductances of these complexes are all above 100 S cm^2 mol^{-1}, which indicates that the complexes are ionic in solution.

4. Conclusions

The π-electron donor *N*-methylacridine forms 2:1 salts with the transition metal complex counterions $[M(mnt)_2]^{2-}$ (M = Ni(II), Zn(II), Cu(II), Cd(II)), and two crystal structures were determined by single crystal X-ray diffraction. The salts show a set of *B*-bands at about 260 nm and a series of *Q*-bands in 400–500 nm regions in the UV–Vis spectra, which probably originated from M–L or L–M transitions. When excited at 350 nm, all the compounds exhibit 480–510 nm emissions, and their fluorescent intensities decrease in the

order: Zn > Cd > Ni > Cu. Compressed pellets of the complexes show specific electrical conductivities at about 10^{-5} S cm^{-1}, which indicate their potential as molecular materials for semiconductors.

5. Supplementary data

Copies of this information may be obtained free of charge from the Director, CCDC, 12 Union Road, Cambridge CB2 1EZ, UK (fax: +44-1223-336-033; e-mail: deposit@ccdc.cam.ac.uk or www: http://www.ccdc.cam.ac.uk) quoting the deposition Nos. 198675 and 198676.

Acknowledgements

The authors thank Prof. Jing Shi and his graduates in the Physics Department of Wuhan University for conductivity measurements.

References

[1] V. Gama, R.T. Henriques, G. Bonfait, L.C. Pereira, J.C. Waerenborgh, I.C. Santos, T. Duarte, J.M.P. Cabral, M. Almeida, Inorg. Chem. 31 (1992) 2598.
[2] Y.S.J. Veldhuizen, W.J.J. Smeets, N. Veldman, A.L. Spek, C. Faulmann, P. Auban-Senzier, D. Jérome, P.M. Paulus, J.G. Haasnoot, J. Reedijk, Inorg. Chem. 36 (1997) 4930.
[3] F. guyon, D. Lucas, I.V. Jourdain, M. Fourmigue, Y. Mugnier, H. Cattey, Organometallics 20 (2001) 2421.
[4] C.T. Vance, R.D. Bereman, J. Bordner, W.E. Hatfield, J.H. Helms, Inorg. Chem. 24 (1985) 2905.
[5] (a) G. Bähr, G. Schleitzer, Chem Ber. 90 (1957) 438;
(b) H.E. Simmons, D.C. Blomstrom, R.D. Vest, J. Am. Chem. Soc. 84 (1962) 4746.
[6] E. Billig, R. Williams, I. Bernal, J.H. Waters, H.B. Gray, Inorg. Chem. 3 (1964) 663.
[7] Y. Kashimura, Y. Okano, J. Yamaura, R. Kato, Synth. Met. 103 (1999) 2123.
[8] J.P. Cornelissen, E.J. Creyghton, R.A.G. de Graaff, J.G. Haasnoot, J. Reedijk, Inorg. Chim. Acta 185 (1991) 97.
[9] C. Mahadevan, M. Seshasayee, B.V. Murthy, P. Kuppusamy, P.T. Manoharan, Acta Crystallogr. A Sect. C 40 (1984) 2032.
[10] H. Endres, H.J. Keller, W. Moroni, D. Nothe, Acta Crystallogr. A Sect. B 35 (1979) 353.
[11] S.P. Best, S.A. Ciniawsky, R.J.H. Clark, R.C.S. Mcqueen, J. Chem. Soc., Dalton Trans. (1993) 2267.
[12] G.R. Lewis, I. Dance, J. Chem. Soc., Dalton Trans. (2000) 3176.
[13] E. Ribera, C. Rovira, J. Veciana, J. Tarrés, E. Canadell, R. Rousseau, E. Molins, M. Mas, J.P. Schoeffel, J.P. Pouget, J. Morgado, R.T. Henriques, M. Almeida, Chem. Eur. J. 5 (1999) 2025.
[14] N. Singh, V.K. Singh, Int. J. Inorg. Mater. 2 (2000) 167.
[15] J.A. Zuleta, J.M. Bevilacqua, D.M. Proserpio, P.D. Harvey, R. Eisenberg, Inorg. Chem. 31 (1992) 2396.
[16] G. Shmauch, F. Knoch, H. Kisch, Chem. Ber. 128 (1995) 303.
[17] J. Bremi, V. Gramlich, W. Caseri, P. Smith, Inorg. Chim. Acta 322 (2001) 23.
[18] V.J. Koester, Chem. Phys. Lett. 32 (1975) 575.
[19] J.A. Zuleta, M.S. Burberry, R. Eisenberg, Coord. Chem. Rev. 97 (1990) 47.
[20] R. Benedix, H. Hennig, H. Kunkely, A. Vogler, Chem. Phys. Lett. 175 (1990) 483.
[21] A. Vogler, H. Kunkely, J. Am. Chem. Soc. 103 (1981) 1559.
[22] H. Kisch, B. Eisen, R. Dinnebier, K. Shankland, W.I.F. David, F. Knoch, Chem. Eur. J. 7 (2001) 738.